doi:10.3788/gzxb20164504.0414001

膨胀石墨制备及其 1.064 μm 激光消光性能

李晓霞[1,2],赵纪金[3],马德跃[1,2],郭宇翔[1,2]
(1 脉冲功率激光技术国家重点实验室,电子工程学院,合肥 230037)
(2 安徽省红外与低温等离子体重点实验室,合肥 230037)
(3 北京遥感研究所,北京 100192)

摘 要:基于两步氧化插层先驱体法制备了不同膨胀体积的膨胀石墨,分析了先驱体、膨胀石墨的微观结构和微观形貌;利用静态测试系统测试了膨胀石墨对 1.064 μm 激光的消光行为,据此计算了其对 1.064 μm 激光的质量消光系数,得到了该系数与膨胀体积的依赖关系,并从消光机理进行了原因分析。结果表明:通过控制和优化先驱体合成条件,可以制得膨胀体积高达 600 mL·g^{-1} 的膨胀石墨;两步插层导致先驱体的层间距(d_{002})明显大于天然石墨,当其 d_{002} 从 0.359 0 nm 增至 0.371 1 nm 时,所得膨胀石墨的膨胀体积从 267 mL·g^{-1} 增至 600 mL·g^{-1};膨胀石墨平均质量消光系数与膨胀体积呈近似线性关系,当膨胀体积由 233 mL·g^{-1} 增至 600 mL·g^{-1} 时,该系数从 0.20 m^2·g^{-1} 升至 0.48 m^2·g^{-1};膨胀石墨对 1.064 μm 激光呈非选择性散射,膨胀体积大,导致几何面积大,对 1.064 μm 激光的散射能力增强;同时,膨胀石墨中出现了更深的孔隙或孔腔,可作为等效黑体增强对入射激光的吸收.

关键词:膨胀石墨;消光;激光;两步氧化插层法;膨胀体积;微观形貌
中图分类号:TN97 **文献标识码**:A **文章编号**:1004-4213(2016)04-0414001-6

Preparation and Extinction Behaviour of Expanded Graphite to 1.064 Micrometer Laser

LI Xiao-xia[1,2], ZHAO Ji-jin[3], MA De-yue[1,2], GUO Yu-xiang[1,2]
(1 *State Key Laboratory of Pulsed Power Laser Technology, Electronic Engineering Institute, Hefei* 230037, *China*)
(2 *Key Laboratory of Infrared and Low Temperature Plasma of Anhui Province, Hefei* 230037, *China*)
(3 *Beijing Institute of Remote Sensing, Beijing* 100192, *China*)

Abstract: A series of Expanded Graphite (EG) with different Expanding Volume (EV) were prepared by the two-step chemical intercalation, and the microstructures and morphologies of the EG particles and their precursors were obtained by X-Ray Diffraction (XRD), Scanning Electron Microscope (SEM) and a stereoscopic microscope, respectively. The extinction behaviour of EG for 1.064 μm laser was measured by a static test, and then the average mass extinction coefficient was calculated and its dependence on EV was obtained and subsequently analyzed by the extinction theory. The results show that EG particles with different EV, especially with an EV of 600 mL·g^{-1}, may be prepared by controlling the synthesis conditions of the precursors, namely graphite intercalation compounds. The average interlayer spacing (d_{002}) of the precursor for EG becomes larger than that of Natural Graphite (NG) due to the two-step intercalation, and the EV of the EG whose precursor's d_{002} rises from 0.3590nm up to 0.3711nm, increases from 267 mL·g^{-1} to 600 mL·g^{-1}. The average mass extinction coefficient of EG depends near-linearly on its EV, and rises from 0.20 m^2·g^{-1} up to 0.48 m^2·g^{-1} while the EV increases from 233 mL·g^{-1} up to 600 mL·g^{-1} in the static test. The phenomenon of nonselective scattering occurs when an incident 1.064 μm laser reaches to EG particles, and then the larger is the surface area of an EG particle owing to a higher EV, the stronger is its scattering power to 1.064 μm laser. Meanwhile, much

Foundation item: The State Key Laboratory of Pulsed Power Laser Technology (No. SKL20132R03)
First author: LI Xiao-xia (1969—), female, professor, Ph. D. degree, mainly focuses on electro-optical materials. Email: lxxhong@aliyun.com
Received: Dec. 30, 2015; **Accepted**: Feb. 24, 2016

deeper pores and cavities appear with the EV increasing, and may work as equivalent black bodies to improve EG absorption of the incident laser.

Key words: Expanded graphite; Extinction; Laser; Two-step chemical intercalation; Expanding volume; Micro morphology

OCIS Codes: 140.3380;160.4670;290.2200;180.5810;120.7000;290.5850

0 Introduction

Expanded Graphite (EG), also termed as exfoliated graphite, is a promising material for many applications including gasket, electrodes, thermal insulator, fire-resistant composites and conductive resin composites[1-2] *etc*. Such material also exhibits excellent adsorption performance for the spilled oil in water, heavy oils or other organics[3-4] *etc*. Recently, EG attracts attention as a helpful precursor for graphene[5-6]. It is also reported that EG has good extinction performance in infrared[7-9], millimeter wave[10], microwave[11] and laser wavebands[12-13].

EG, a kind of modified graphite, is usually prepared from Graphite Intercalation Compounds (GIC) by rapid heating (usually up to 600～1000℃), and GIC is synthesized by the insertion of a wide range of atoms, molecules and ions between layers of graphite host materials[14-18]. After expansion, EG consists of high-aspect-ratio vermicular graphitic particles, and has a larger interlayer spacing with a layered structure than natural flake graphite. Therefore, much more pores, galleries and exposed layers occur in EG particles, and may interact with some incident electromagnetic waves[17].

Expanding Volume (EV), or called expanded volume and exfoliation volume, is a common parameter to describe the expanding extent of the resulting EG[15,18], and it has something to do with EG packing density, extinction coefficient and so on. ZHAO Ji-jin *et al*. have concluded that a high EV is benefit to infrared and millimeter wave extinction behavior of EG[8,10]. The extinction coefficients of certain EG particles for 1.06 μm laser have been calculated or measured[12-13].

In spite of the prior work mentioned above, the extinction behavior of EG has not been previously studied with focused on how the laser extinction performance depends on the EV of EG. Therefore, based on our former work [8,10,17-19], some EG particles with several different EV were synthesized in this work, and their extinction behavior for 1.064 μm laser were quantitatively studied, which is instructive to obtain the EG with an excellent laser extinction capability.

1 Material and methods

1.1 Materials

The Natural Graphite (NG) used as host material for preparing EG was purchased from Pengsong Graphite Factory in Pingdu city of China, and it has a purity of 99.9% and an average size of 300 μm. The other reagents used in the experiment, such as sulfuric acid (H_2SO_4), potassium permanganate ($KMnO_4$), perchloric acid ($HClO_4$) and acetic acid (CH_3COOH) are all analytical grade.

1.2 Synthesis of GIC

GIC, the precursor for EG, was synthesized by the following procedures [17-18]. As a first step, 5 g of pure natural flake graphite, 10～30 mL of $HClO_4$ (70～72%), and 0.5～2 g of $KMnO_4$ were added into a three-necked flask. The mixture was heated and kept stirring at 25℃ for about 50 minutes. After reacting sufficiently, the resulting product was washed with distilled water three times, and subsequently dried under vacuum at 40℃, and then pre-GIC was obtained.

In the second step, 10～30 mL of CH_3COOH and 10～30 mL of $HClO_4$ were poured into the flask where there was 5 g of pre-GIC, and then 0.8～1.2 g of $KMnO_4$ was added too. We obtained GIC after the procedures of heating, stirring, washing, and drying, as mentioned above.

Therefore, a series of GIC were synthesized according to controlling the usage ratio of raw graphite to intercalator and oxidant.

1.3 Synthesis of EG from GIC

Each sample of GIC (2～3g) synthesized under different reaction conditions, was put into a certain crucible, respectively. And then the crucibles were placed in a vertical muffle furnace preheated above 800℃ for 20～30s. After that, EG samples with different EV were prepared successively.

1.4 Characterization and measurement

Micro morphology images of NG, pre-GIC, GIC and EG particles were obtained on a JEOL JSM-6700F Scanning Electron Microscope (SEM). The whole morphology of an EG particle was obtained on an XTL-3400 stereoscopic microscope (×20～3100). Expanding volume or bulk density was determined by expanding the precursor and measuring the volume which a given mass of EG occupies in a measuring cylinder[20]. The XRD patterns of samples were analyzed on a Shimadzu XRD-7000 diffractometer (CuKa radiation, $\lambda=0.154\ 18$ nm; 60 kV, 80 mA; scanning range $2\theta=20\sim80°$; scanning rate 4°/min;

anodic voltage 60 kV and current 80 mA).

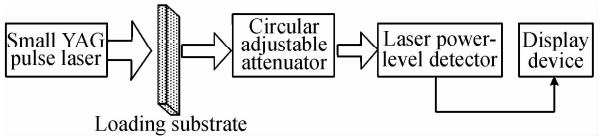

Fig. 1 Schematic arrangement of a static testing way

The extinction behavior of the obtained EG was characterized by testing its laser transmission and extinction coefficient by a static testing way [21], which is the easiest way to collect and suspend particles on a transparent substrate while smoke chamber trials are costly and time consuming. The schematic arrangement for the static test is illustrated in Fig. 1, where a transparent adhesive substrate (18cm × 18cm) was placed in line between a small Yttrium Aluminum Garnet (YAG) laser (Power, pulse width and frequency were 20mJ, 15ns and 1Hz, respectively.) and a round GCO-303004 adjustable attenuator which was followed by a LE-3 laser power-level detector. In addition, 100±0.1 mg of EG was evenly dispersed and adhered to the substrate as a specimen.

The transmission through the specimen or the reference blank was measured on 18 sites of a loading substrate at a time. In term of a blank substrate, the value shown on the display was recorded 18 times and then produced an average value in order to reduce measurement errors. This average value was referred as the reference blank transmission $\bar{E}_0$. When the substrate was loaded with EG with a certain EV, the value shown on the display was similarly recorded 18 times and then achieved an average value $\bar{E}$ too, which was referred as the transmission of a certain EG sample.

2 Results and discussion

2.1 Morphologies of NG, pre-GIC and GIC

The SEM micrographs of NG, pre-GIC and the resulting GIC are shown in Fig. 2. The SEM images demonstrate clearly the morphological variation of graphite before and after intercalation. The NG layers shown in Fig. 2(a) are tightly in contact with each other, and the interlayer spacing is very small, and that of pre-GIC becomes a little larger owing to the first step oxidation and intercalation (Fig. 2(b)). Meanwhile, as shown in Fig. 2(c)~(f), much more and larger interlayer spacing appear in the GIC as the precursor for EG with an EV of 267, 383, 510 and 600 mL·g^{-1}, respectively. It is obvious that the precursor for EG with a higher EV often has much more and larger interlayer spacing.

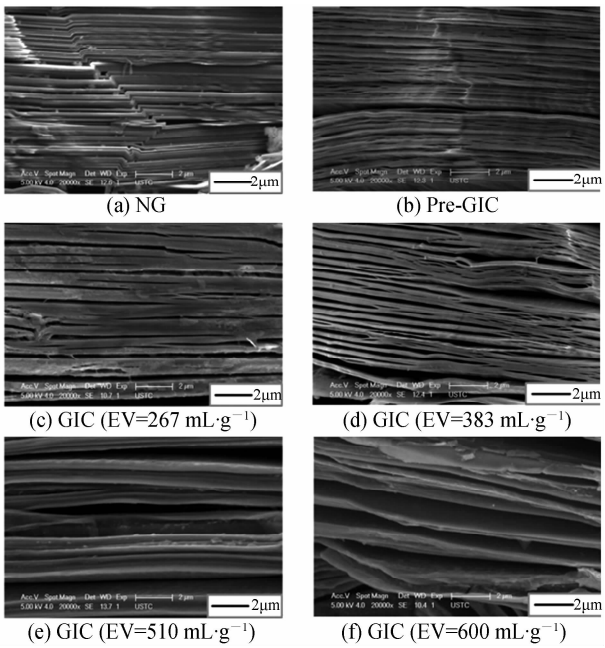

Fig. 2 SEM images of NG, pre-GIC and GICs

2.2 XRD patterns of NG, pre-GIC and GIC

The XRD patterns of NG, pre-GIC and GIC are presented in Fig. 3, and the 2θ of $(00l)$ peaks and the d-spacing (d_{00l}) values are listed in Table 1. It can be seen that the average interlayer spacing of the pre-GIC d_{002} is 0.3556 nm for the (002) peak at $2\theta=25.02°$, and this value is somewhat higher than that for NG whose d_{002} value is 0.3358 nm at $2\theta=26.52°$. As the EV of EG particles increases from 267 to 600 mL·g^{-1}, the d_{002} value of the precursor GIC for the (002) peak rises from 0.359 0 nm up to 0.371 1 nm while 2θ drops from 24.78° to 23.96°.

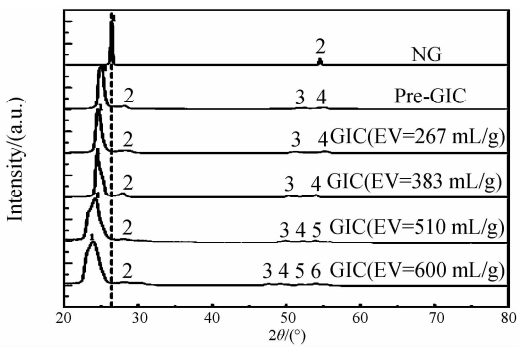

Fig. 3 XRD patterns of NG, pre-GIC and GICs

According to the Bragg equation, the higher is the interlayer spacing, the lower is the value of 2θ. Therefore, the pre-GIC obtained by the intercalation of $HClO_4$ into NG in step 1 leads to an increase of interlayer spacing along c-axis, and the GIC obtained by the intercalation of CH_3COOH into pre-GIC in step 2 leads to a higher d-spacing (d_{00l}) value. The increased interlayer distance for the GIC may be helpful

for the intercalation of much more atoms, molecules and ions. So the GIC with a higher d-spacing (d_{00l}) value will become expanded enough and get EG with a higher EV because of the decomposition of more intercalation compounds during the thermal shock.

Table 1 Values of 2θ and d-spacing (d_{00l}) from XRD patterns of NG, pre-GIC and GICs

Sample	Peak number	2θ/(°)	d/nm
NG	1	26.52	0.335 8
	2	54.64	0.167 8
Pre-GIC	1	25.02	0.355 6
	2	28.04	0.317 9
	3	51.44	0.177 5
	4	56.36	0.163 1
GIC (EV=267 mL·g^{-1})	1	24.78	0.359 0
	2	28.24	0.315 7
	3	50.88	0.179 2
	4	56.32	0.163 2
GIC (EV=383 mL·g^{-1})	1	24.48	0.363 3
	2	28.00	0.318 4
	3	50.24	0.184 1
	4	54.12	0.169 3
GIC (EV=510 mL·g^{-1})	1	24.28	0.366 3
	2	28.16	0.316 6
	3	49.84	0.182 8
	4	52.32	0.174 7
	5	54.04	0.169 6
GIC (EV=600 mL·g^{-1})	1	23.96	0.371 1
	2	28.12	0.317 1
	3	47.76	0.190 2
	4	49.12	0.185 3
	5	51.88	0.176 1
	6	53.96	0.169 8

2.3 Morphologies of EG with different EV

For the whole view of an EG particle, the stereoscopic images of EG with different EV are shown in Fig. 4. It can be seen that an EG particle has a length of several millimeters, and a diameter of about hundreds of micrometers. The EG particle with a higher EV is much longer than that with a lower one.

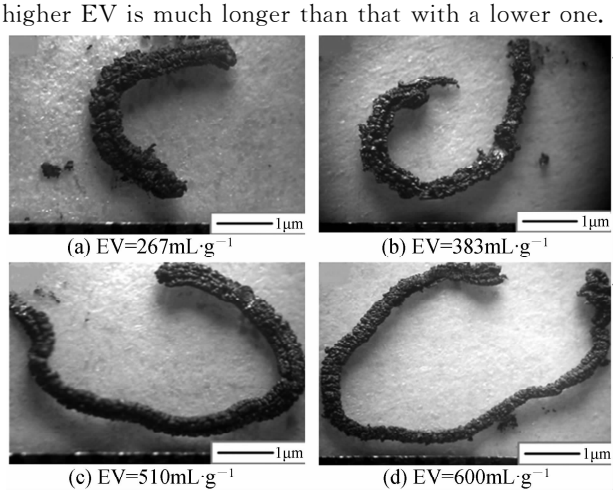

Fig. 4 Stereoscopic microscope images of EG particles

SEM images of EG with different EV are shown in Fig. 5. It is obvious that EG has a cellular structure (an accordion-like structure) and consists of cell walls and voids. As shown in the upper-right corner of Fig. 5, much more and deeper pores appear with the increase of EV.

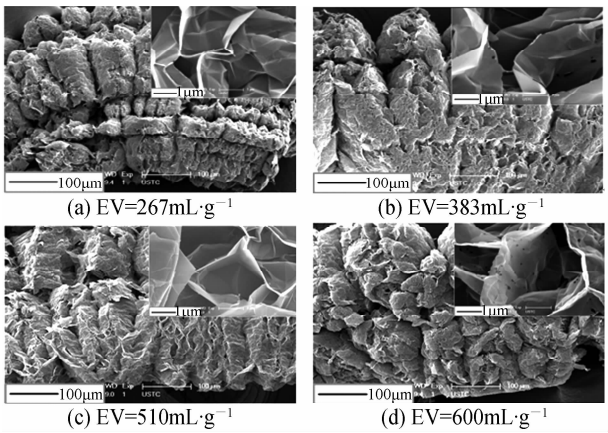

Fig. 5 SEM images of EG with different EVs

2.4 Laser extinction behavior of EG

After the static testing shown in Fig. 1, the average value of the reference blank transmission $\bar{E}_0$ is 0.91 mJ. And those of the sample transmission $\bar{E}$ for EG with a certain EV or bulk density, are also obtained. Therefore, the transmittance τ of EG particles to the incident light, as shown in Eq. (1), can be achieved from the ratio of each sample transmission $\bar{E}$ to the average reference blank transmission $\bar{E}_0$. The data are listed in table 1.

$$\tau=\frac{\bar{E}}{\bar{E}_0}\times 100\% \tag{1}$$

As seen in Table 2, the EG with an EV of 600 mL·g^{-1} is prepared by two-step chemical intercalation in this work, and the maximum of EV is higher than 450 mL·g^{-1} or 550 mL·g^{-1} reported in prior work[10,22]. When an incident 1.064 μm laser traverses EG particles suspended on a transparent substrate, the beam transmittance τ drops away with the increasing of EV, and the value of τ falls down from 53.85% to 23.08% while that of EV rises from 233 mL·g^{-1} to 600 mL·g^{-1}.

The mass extinction coefficient of particles, σ_M defined as extinction section per unit mass, is an intrinsic physical parameter to character the shielding property of passive interfering materials. A high value of σ_M often corresponds to a good extinction performance. The relation between τ and σ_M can be formulated by Lambert-Beer law shown in Eq. (2)

$$\tau=\exp(-\sigma_M C_m L) \tag{2}$$

where C_m(g·m^{-3}) is the mass concentration of particles along the line of sight, and L (m) is the path-length. The quantity $C_m L$(g·m^{-2}) is the column density, namely, the particle mass per unit area in light path.

Table 2 Transmittance τ of EG particles with different EV or bulk density ρ

EG	EV/(mL·g^{-1})	ρ/(mg·mL^{-1})	$\bar{E}$/mJ	τ/%
1	233	4.29	0.49	53.85
2	267	3.75	0.44	48.35
3	300	3.33	0.41	45.05
4	330	3.03	0.39	42.86
5	366	2.73	0.36	39.56
6	395	2.53	0.33	36.26
7	410	2.44	0.31	34.06
8	430	2.33	0.30	32.97
9	450	2.22	0.28	30.77
10	480	2.08	0.27	29.67
11	510	1.96	0.26	28.57
12	550	1.82	0.24	26.37
13	568	1.76	0.23	25.27
14	600	1.67	0.21	23.08

* Footnote: $\bar{E}_0$ is 0.91 mJ.

Based on Eqs. (1) and (2), the σ_M becomes

$$\sigma_M = \frac{1}{C_m L}\ln\frac{1}{\tau} = \frac{1}{C_m L}\ln\frac{\bar{E}_0}{\bar{E}} \tag{3}$$

This equation provides a convenient and compatible set of units with beam. Values of σ_M and EV, and the σ_M-EV curve are represented in Fig. 6, which demonstrate that the values of σ_M near-linearly depend on those of EV, and σ_M increases near-linearly from 0.200 6 m^2·g^{-1} to 0.475 1 m^2·g^{-1} while EV rises from 233 mL·g^{-1} up to 600 mL·g^{-1}.

The values of σ_M obtained from the static testing method are smaller than that gotten in a smoke chamber [12]. One reason is that the EG in this work may have different extinction performance from that measured in the prior work due to their different sources [12]. The other is that the distribution of EG particles along the line of sight is different each other. Under static testing conditions, only a single EG particle or a thin layer of them adheres to the adhesive substrate and interacts with an incident laser, while many EG particles in a laser path can do so in a smoke chamber. The static testing results may describe the extinction behavior of an EG particle with a certain expanding state.

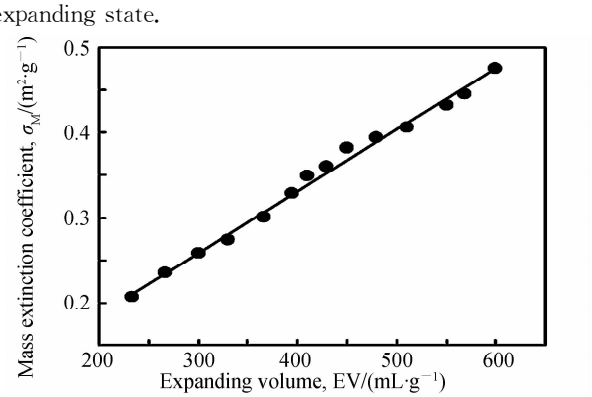

Fig. 6 Dependence of mass extinction coefficient on EV

The extinction coefficient is defined in terms of the beam attenuation of electromagnetic radiation due to scattering and absorption as the beam traverses a medium. Beam attenuation depends on the complex refractive index, size, shape, orientation and concentration of particles, as well as the wavelength and polarization of incident radiation. In this test, the size and shape of an EG particle are different each other owing to different EV, as shown in Fig. 4 and Fig. 5.

As a special kind of graphite, EG is somewhat conductive and has a good electromagnetic scattering power. Scattering factor μ_s can be expressed as follows [23]

$$\mu_s = \pi \cdot a^2 \cdot K \cdot n \tag{4}$$

where a is section radius, K is scattering area index and depends on electro size a/λ (λ is the wavelength of an incident electromagnetic wave), n is the number of scattering bodies.

For a scattering body, when the value of a is close or equal to that of λ, K reaches the maximum and a strong scattering called Mie scattering occurs. If the value of a is much greater than that of λ, K may be regarded as a constant, and nonselective scattering happens, where μ_s is directly proportional with the area πa^2 and the number n of scattering bodies. It is demonstrable that more and larger geometry sections are good for a high scattering power.

From the stereoscopic images (in Fig. 4) of an EG particle with different EV, it can be seen that the size of an EG particle is much greater than 1.064 μm (the wavelength of an incident laser), and then nonselective scattering occurs. Therefore, the larger is the surface area of an EG particle due to a higher EV, the greater is the scattering factor μ_s, and the stronger is the scattering power of EG particles.

EG exhibits good absorption for oil as well as electromagnetic waves due to its cellular structure. The void (or cell) can be viewed as a small cavity whose size is approximate to a few microns (in Fig. 5) which is fit with infrared wavelength. Based on Cavity Theory, the cavity absorptivity α in infrared region, can be expressed in Eq. (5)

$$\alpha = 1 - \rho\frac{\pi \cdot r^2}{L^2} \tag{5}$$

where ρ is the reflectivity of cavity walls, r is the aperture radius of a cavity, and L is the cavity depth.

The higher is the value of L/r, the higher is the cavity absorptivity. Therefore, deeper pores and voids which may work as equivalent black bodies are good for improving the electromagnetic wave absorptivity of EG. It can be seen in the upper-right corner of Fig. 5 that EG with a higher EV usually has much deeper pores and galleries than that with a lower EV.

4 Conclusions

A series of EG particles with different EV, especially with an EV of 600 mL · g^{-1}, may be prepared by the two-step chemical intercalation by controlling the synthesis conditions of the precursor GIC. The average interlayer spacing (d_{002}) of the pre-GIC and GIC becomes larger and larger than that of NG due to the intercalation of $HClO_4$ into NG in step1 and CH_3COOH into pre-GIC in Step 2.

The average mass extinction coefficient of EG is near-linearly dependent on EV, which means that EG with a high EV have good laser extinction performance. The phenomenon of nonselective scattering occurs when an incident 1.064 μm laser reaches EG particles for the physical dimension of an EG particle is much greater than 1.064 μm. And the larger is the surface area of an EG particle owing to a higher EV, the stronger is its scattering power to 1.064 μm laser. Meanwhile, much deeper pores and cavities appear with the EV increase, and may work as equivalent black bodies to improve EG absorption of the incident laser.

The preparation and application of EG particles with higher EV and better laser extinction behavior may be researched in the further work.

Reference

[1] CHUNG D D. Flexible graphite for gasketing, adsorption, electromagnetic interference shielding, vibration damping, electrochemical applications, and stress sensing[J]. *Journal of Materials Engeering and Performance*, 2000, **9**(2):161-163.

[2] SONG S H, JEONG H K, KANG Y G. Preparation and characterization of expanded graphite and its styrene butadiene rubber nanocomposites[J]. *Journal of Industrial and Engeering Chemistry*, 2010, **16**:1059-1065.

[3] ZHENG Y P, WANG H N, KANG F Y, *et al*. Sorption capacity of expanded graphite for oils-sorption in and among worm-like particles[J]. *Carbon*, 2004, **42**:2603-2607.

[4] VIEIRA F, CISNEROS I, ROSA N G, *et al*. Influence of the natural flake graphite particle size on the textural characteristic of expanded graphite used for heavy oil sorption[J]. *Carbon*, 2006, **44**(12):2590-2592.

[5] GRAYFER E D, NAZAROV A S, MAKOTCHENKO V G, *et al*. Chemic ally modified graphene sheets by functionalization of highly expanded graphite[J]. *Journal of Material Chemistry*, 2011, **21**(10):3410-3414.

[6] GRAYFER E D, Nazarov A S, MAKOTCHENKO V G, *et al*. Highly expanded graphite as a precursor for graphene materials[C]. IEEE Conference Publishing, 2007, 375-376.

[7] DOU Zheng-wei, LI Xiao-xia, ZHAO Ji-jin. Research on complex refraction indices of expanded graphite[J]. *Journal of China Ordnance*, 2011, **7**(4):243-247.

[8] ZHAO Ji-jin, LI Xiao-xia, GUO Yu-xiang, *et al*. Effect of expanding volume of expanded graphite on infrared screening performance[J]. *Infrared and Laser Engineering*, 2014, **43**(2):434-437.

[9] BA Shu-hong, JIANG Chun-hong, SUN Kang-bo, *et al*. Prepared and infrared extinction characteristics of micron expanded graphite[J]. *Advanced Materials Research*, 2011, (308-310):710-714.

[10] ZHAO Ji-jin, LI Xiao-xia, GUO Yu-xiang, *et al*. Effect of expanding volume of expanded graphite on millimeter-wave attenuation performance[J]. *Acta Photonica Sinica*, 2014, **43**(3):03160031.

[11] GOGOI J P, BHATTACHARYYA N S. Microwave characterization of expanded graphite/phenolic resin composite for strategic applications, extended abstracts[C]. Progress in Electromagnetics Research Symposium (Kuala Lumpur, Malaysia): Telekom Malaysia, 2012, 1880-1884.

[12] WANG Xuan-yu, PAN Gong-pei. Extinction performance of superfine graphite smoke to 10.6 μm laser emission[C]. 2nd International Symp on Adv Optical Manufac and Testing Tech: Optical Test and Measurement Tech and Equip, Proceedings of SPIE, 2006, 6150:2R-1-6.

[13] YAO Yong-ping. Study on extinction characteristics of expanded graphite smoke to1.06 and 10.6 μm laser[J]. *Pyrotechnics*, 2011, (1):42-45.

[14] LI Ji-hui, LIU Qian, DA Hui-fang. Preparation of sulfur-free expanded graphite at a low exfoliation temperature[J]. *Materials Letters*, 2007, **61**:1832-1834.

[15] YU Xiu-Juan, WU Juan, ZHAO Qi, *et al*. Preparation and characterization of sulfur-free expanded graphite with large expanded volume[J]. *Materials Letters*, 2012, **73**:11-13.

[16] SAIDAMINOV M I, MAKSIMOVA N V, SOROKINA N E, *et al*. Effect of graphite nitrate exfoliation conditions on the released gas composition and properties of expanded graphite[J]. *Inorganic Materials*, 2013, **49**(9):883-888.

[17] ZHAO Ji-jin, LI Xiao-xia, GUO Yu-xiang, *et al*. Preparation and microstructure of two kinds of expanded graphite[J]. *Advanced Materials Research*, 2013, (706-708):211-214.

[18] ZHAO Ji-jin, LI Xiao-xia, GUO Yu-xiang, *et al*. Preparation and microstructure of expanded graphite with large expanding volume by two-step intercalation[J]. *Advanced Materials Research*, 2014, **852**:101-105.

[19] ZHAO Ji-jin. Theoretical and experimental investigation of multiple-band passive screening materials[D]. Electronic Engineering nstitute, Hefei, China, 2014.

[20] MAKOTCHENKO V G, GRAYFER E D, NAZAROV A S, *et al*. The synthesis and properties of highly exfoliated graphites from fluorinated graphite intercalation compounds[J]. *Carbon*, 2011, **49**(10):3233-3241.

[21] HUFFMAN D R. Extinction measurements on aluminum and carbon smoke particles from far infrared to far ultraviolet[P]. *AD-A*179003, 1987.

[22] WEI Xing-hai, LIU Lang, ZHANG Jin-xi, *et al*. The preparation and morphology characteristics of exfoliated graphite derived from $HClO_4$-graphite intercalation compounds[J]. *Materials Letters*, 2010, **64**:1007-1009.

[23] MA De-yue, LI Xiao-xia, GUO Yu-xiang, *et al*. Effect of preforming pressure to precursor on the propertty of exfoliated graphite[J]. *Acta Photonica Sinica*, 2015, **44**(3):03310031.